Nonprehensile manipulation of an underactuated mechanical system with second order nonholonomic constraints: the robotic hula-hoop

Alejandro Gutiérrez–Giles, Fabio Ruggiero, Vincenzo Lippiello, and Bruno Siciliano

***Abstract*—A mechanical system consisting of a hoop and a pole is considered, for which the corresponding dynamic model represents an underactuated system subject to second-order nonholonomic constraints. The pursued goal is to simultaneously track a trajectory in the unactuated coordinates and to stabilize the actuated ones. For the model under consideration, the well-known noncollocated partial feedback linearization algorithm fails since the corresponding zero dynamics is unstable. In this work, we show that the actuated coordinates, *i.e.,* the pole can be stabilized by exploiting the null space of the coupling inertia matrix without affecting the performance in the underactuated coordinates tracking. We present a formal mathematical analysis, which guarantees ultimate boundedness of all coordinates. Performed simulations bolster the proposed approach.**

***Index Terms*—Nonholonomic Mechanisms and Systems, Motion Control, Dynamics, Underactuated Robots**

I. INTRODUCTION

MANY applications that involve manipulating an object with a robotic system carry out this task in a *prehensile* way, *e.g.,* pick and place. Alternatively, this manipulation can be made in a *nonprehensile* fashion [1]. Nonprehensile manipulation has the advantage of extending the robot workspace and the number of tasks that can be performed with the same robot kinematics. Nevertheless, these advantages come along with a considerable increase in the complexity of the design of suitable control strategies. To deal with complex nonprehensile tasks, they are usually decomposed into simpler basic sub-tasks called *nonprehensile manipulation primitives*. Such primitives include rolling [2], batting [3], pushing [4], throwing [5], sliding [6], and so on. Several of these primitives often involve unilateral control inputs, *e.g.,* the actuator can only push the object but cannot pull it, which complicates even more the controller design. Additionally, in nonprehensile manipulation problems, not only the dynamic but the geometric properties of both the object and the robot end-effector are important at the trajectory planning and controller designing stages [7].

In this paper, we consider an example of the rolling primitive, *i.e.,* a hoop and a pole system, where only the pole is actuated. Our goal is to induce a constant spinning of the hoop around the pole on a desired position over the pole surface while maintaining a stable pole motion. In the context of the rolling primitive, most works consider only planar movement, with holonomic kinematic constraints [8], [9], [10]. In contrast, the problem treated here is a mechanical underactuated system subject to nonholonomic constraints evolving in the 3D Cartesian space. Furthermore, contrarily to [11] and [12], we have solved the pole drifting problem.

To design a control strategy we assume that a kinematic and a dynamic model obtained by means of the Montana's equations and the Lagrange–d'Alembert formulation (as in [12]), are available. However, in this work we do not assume *a priori* which coordinates of the pole are actuated, but we carry out an analysis to compare among several possible choices. We also assume that the pole motion can be provided by a robotic system, as the one depicted in Fig. 1[1], which has the additional advantage of a possible change of the pole apparent dynamics. By exploiting the particular properties of the model, we divide the control input in two parts, one which affects the hoop motion and another that does not affect it. Then, we first design a nonlinear controller to satisfy the control objective for the hoop coordinates and later we employ a LQR controller to locally stabilize the pole motion.

II. MODEL AND PROPERTIES

Consider the hoop and pole system shown in Fig. 1. Let the orthonormal frames $o_{\mathrm{w}}x_{\mathrm{w}}y_{\mathrm{w}}z_{\mathrm{w}}$ be the inertial frame, $o_{\mathrm{p}}x_{\mathrm{p}}y_{\mathrm{p}}z_{\mathrm{p}}$ a frame attached to the pole, $o_{\mathrm{h}}x_{\mathrm{h}}y_{\mathrm{h}}z_{\mathrm{h}}$ a frame attached to the hoop, and $o_{\mathrm{c}}x_{\mathrm{c}}y_{\mathrm{c}}z_{\mathrm{c}}$ the contact frame defined as follows: $\boldsymbol{o}_{\mathrm{c}}$ is the contact point, $\boldsymbol{x}_{\mathrm{c}}$ is a vector passing through the contact point and pointing outwards the pole surface, $\boldsymbol{y}_{\mathrm{c}}$ a vector in the intersection of the pole surface tangent plane at the contact point and the hoop equatorial plane, and $\boldsymbol{z}_{\mathrm{c}}$ defined to form an orthonormal frame.

The contact kinematics can be obtained by employing local coordinates, *i.e.,* the pole surface coordinates $z_{\mathrm{o}} \in \mathbb{R}$ and $\theta \in \mathbb{R}$, the hoop surface coordinates $\gamma \in \mathbb{R}$ and $\psi \in \mathbb{R}$, and the relative rotation coordinate $\phi \in \mathbb{R}$ described as follows [12]:

Manuscript received: August, 1, 2017; Revised October, 21, 2017; Accepted December, 31, 2017.

This paper was recommended for publication by Editor Tamim Asfour upon evaluation of the Associate Editor and Reviewers' comments. This work was partially supported by the RoDyMan project, which has received funding from the European Research Council FP7 Ideas under Advanced Grant agreement number 320992. The authors are solely responsible for the content of this manuscript.

The authors are with CREATE Consortium and Prisma Lab. Department of Electrical Engineering and Information Technology, University of Naples Federico II, Via Claudio 21, 80125, Naples, Italy. {giles.gutierrez, fabio.ruggiero, vincenzo.lippiello, bruno.siciliano }@unina.it

Digital Object Identifier (DOI): see top of this page.

[1]The actual humanoid-like robot is available at the PRISMA Lab and is a part of the RoDyMan project (www.rodyman.eu).

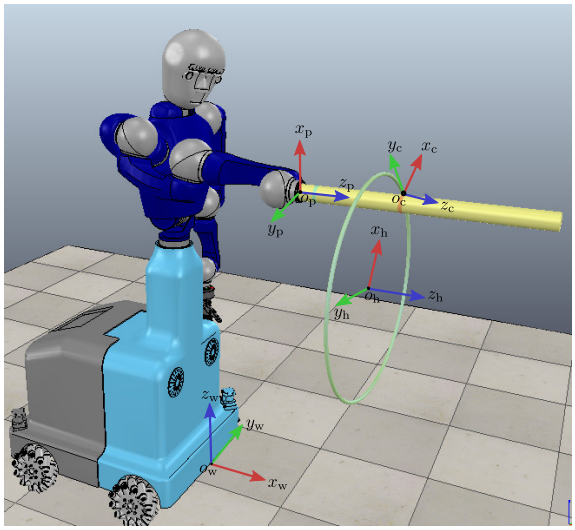

Fig. 1. Pole and hoop system.

- z_o is the distance to the contact point measured over the $\boldsymbol{z}_\mathrm{p}$ axis.
- θ is the angle from one arbitrary point on the pole surface to the contact point measured over the $\boldsymbol{z}_\mathrm{p}$ axis.
- γ is the angle from one arbitrary point on the hoop surface to the contact point over the $\boldsymbol{z}_\mathrm{h}$ axis.
- ψ is the angle from an arbitrary point on the equator of the hoop to the contact point measured over the $\boldsymbol{y}_\mathrm{c}$ axis.
- ϕ is the angle between two tangent vectors, one of each surface, measured over the $\boldsymbol{x}_\mathrm{c}$ axis (see [13, Section 6.2] for details).

Furthermore, we group the contact coordinates in $\boldsymbol{q}_\mathrm{c} \triangleq \begin{bmatrix}\gamma & \psi & z_\mathrm{o} & \theta & \phi\end{bmatrix}^\mathrm{T}$. We denote by $\boldsymbol{q}_\mathrm{p} \in \mathbb{R}^m$ the pole configuration vector, where $m \leq 6$ is the number of pole degrees of freedom. The complete generalized coordinates for the system under consideration are given by the vector $\boldsymbol{q} \triangleq \begin{bmatrix}\boldsymbol{q}_\mathrm{c}\,;\,\boldsymbol{q}_\mathrm{p}\end{bmatrix}$, where $\begin{bmatrix}\boldsymbol{x}\,;\,\boldsymbol{y}\end{bmatrix}$ is a shorthand notation for $\begin{bmatrix}\boldsymbol{x}^\mathrm{T}\,\boldsymbol{y}^\mathrm{T}\end{bmatrix}^\mathrm{T}$. We also define the vector of hoop coordinates $\boldsymbol{q}_\mathrm{h} \triangleq \begin{bmatrix}\gamma & \psi\end{bmatrix}^\mathrm{T}$, which is a subset of $\boldsymbol{q}_\mathrm{c}$, and the vector $\boldsymbol{q}_\mathrm{r} \triangleq \begin{bmatrix}\boldsymbol{q}_\mathrm{h}\,;\,\boldsymbol{q}_\mathrm{p}\end{bmatrix}$. From these definitions and by following the same modeling procedure as in [12], we obtain the dynamic model

$$\boldsymbol{M}_\mathrm{h}(\boldsymbol{q})\ddot{\boldsymbol{q}}_\mathrm{h} + \boldsymbol{c}_\mathrm{h}(\boldsymbol{q},\dot{\boldsymbol{q}}_\mathrm{r}) + \boldsymbol{T}_\mathrm{h}(\boldsymbol{q})\ddot{\boldsymbol{q}}_\mathrm{p} = \boldsymbol{0} \tag{1}$$

$$\boldsymbol{M}_\mathrm{p}(\boldsymbol{q})\ddot{\boldsymbol{q}}_\mathrm{p} + \boldsymbol{c}_\mathrm{p}(\boldsymbol{q},\dot{\boldsymbol{q}}_\mathrm{r}) + \boldsymbol{T}_\mathrm{h}^\mathrm{T}(\boldsymbol{q})\ddot{\boldsymbol{q}}_\mathrm{h} = \boldsymbol{u}\,, \tag{2}$$

subject to the nonholonomic constraints

$$\dot{\theta} = (l_\mathrm{h} c_\phi / r_\mathrm{p})\,\dot{\gamma} \tag{3}$$

$$\dot{z}_\mathrm{o} = -l_\mathrm{h} s_\phi \dot{\gamma} \tag{4}$$

$$\dot{\phi} = -s_\psi \dot{\gamma}\,, \tag{5}$$

where $l_\mathrm{h} > 0$ is the hoop radius, $r_\mathrm{p} > 0$ is the pole radius, and s_x and c_x are shorthand notations for $\sin(x)$ and $\cos(x)$, respectively. In the above equations $\boldsymbol{M}_\mathrm{h}(\boldsymbol{q}) \in \mathbb{R}^{2\times 2}$ and $\boldsymbol{M}_\mathrm{p}(\boldsymbol{q}) \in \mathbb{R}^{m\times m}$ are symmetric positive definite matrices, $\boldsymbol{c}_\mathrm{h}(\boldsymbol{q},\dot{\boldsymbol{q}}_\mathrm{r}) \in \mathbb{R}^2$ and $\boldsymbol{c}_\mathrm{p}(\boldsymbol{q},\dot{\boldsymbol{q}}_\mathrm{r}) \in \mathbb{R}^m$ are vectors accounting for centripetal, Coriolis and gravitational forces, $\boldsymbol{u} \in \mathbb{R}^m$ is the vector of input forces acting on the pole, and $\boldsymbol{T}_\mathrm{h}(\boldsymbol{q}) \in \mathbb{R}^{2\times m}$ is the inertia coupling matrix. If $\mathrm{rank}(\boldsymbol{T}_\mathrm{h}(\boldsymbol{q})) = 2, \forall \boldsymbol{q}$, the underactuated system is said to be *strong inertially coupled* [14]. If the system is strong inertially coupled, the Penrose's right pseudoinverse matrix

$$\boldsymbol{T}_\mathrm{h}^+ \triangleq \boldsymbol{T}_\mathrm{h}^\mathrm{T}\left(\boldsymbol{T}_\mathrm{h}\boldsymbol{T}_\mathrm{h}^\mathrm{T}\right)^{-1} \tag{6}$$

is well defined and therefore we can construct the following orthogonal projection matrices

$$\boldsymbol{P}_\mathrm{h} \triangleq \boldsymbol{T}_\mathrm{h}^+\boldsymbol{T}_\mathrm{h} \tag{7}$$

$$\boldsymbol{Q}_\mathrm{h} \triangleq \boldsymbol{I}_3 - \boldsymbol{P}_\mathrm{h}\,. \tag{8}$$

Notice that $\boldsymbol{P}_\mathrm{h}$ projects every $\mathbb{R}^m$-vector onto the rank space of $\boldsymbol{T}_\mathrm{h}$. Conversely, $\boldsymbol{Q}_\mathrm{h}$ makes the projection into the null space of $\boldsymbol{T}_\mathrm{h}$. It is straightforward to verify that the following relations hold: $\boldsymbol{P}_\mathrm{h}\boldsymbol{T}_\mathrm{h}^\mathrm{T} = \boldsymbol{T}_\mathrm{h}^\mathrm{T}$, $\boldsymbol{T}_\mathrm{h}\boldsymbol{P}_\mathrm{h} = \boldsymbol{T}_\mathrm{h}$, $\boldsymbol{Q}_\mathrm{h}\boldsymbol{T}_\mathrm{h}^\mathrm{T} = \boldsymbol{O}$, and $\boldsymbol{T}_\mathrm{h}\boldsymbol{Q}_\mathrm{h} = \boldsymbol{O}$.

Nonlinear controllability

The controllability of the dynamic system (1)–(2) depends on the actuation of the pole. We have analyzed several configurations of interest (2 rotations, 3 translations, 2 rotations + 2 translations, and 3 rotations + 3 translations) with the aid of a symbolic computing software (*Wolfram Mathematica* [15]). For all the configurations mentioned above, the corresponding dynamic model is strong inertially coupled. Thus, the motivation for comparison is to find the configuration with fewer degrees of freedom having the best controllability properties. The conclusions given below are valid for all the cases mentioned.

First, for the model (1)–(2) the gravity torque in the underactuated part is not constant and the inertia matrix depends on the unactuated variables, so it never fulfills the structural necessary and sufficient conditions given in [16], and the nonholonomic constraints are thus of the *second-order* kind. As a consequence, the dynamic system is *strongly accessible* [17], *i.e.,* in principle, every possible configuration can be reached. However, the strong accessibility property "is far from being sufficient for the existence of a feedback control which asymptotically stabilizes the underactuated system" [17]. For the system (1)–(2), it turns out from [18] that the Brockett's necessary condition for the existence of a continuous asymptotically stabilizing feedback control law is equivalent to check if the image of

$$\mathbf{M}_\mathrm{h}^{-1}(\mathbf{q})\mathbf{c}_\mathrm{h}(\mathbf{q},\dot{\mathbf{q}}_\mathrm{r}) \tag{9}$$

contains a neighborhood of the origin in $\mathbb{R}^{n-m}$. Although the preceding condition is satisfied by all the case studies, it does not imply that there exists such a control law.

A stronger notion of controllability is the so called *small time local controllability* (STLC), which in fact guarantees the existence of a piecewise asymptotic stabilizing feedback control law [19]. For underactuated mechanical systems, the STLC property also guarantees the existence of an asymptotic stabilizing continuous time-periodic controller [20]. A sufficient condition to check the STLC property for mechanical systems is given in [17]. Regrettably, this condition is not met by any of the case studies, and therefore no conclusion

can be made about the STLC property of the system (1)–(2). A necessary and sufficient condition for the STLC is given in [21]. Unfortunately, this condition is much more difficult to check even with the help of symbolic computing software.

Finally, the control design and the subsequent analysis can be simplified by transforming the system into a *normal form* as proposed in [22]. Once again, this sufficient condition is not met by any of the cases under consideration.

Challenges from the control perspective

The control objective is to spin the hoop at a desired constant angular velocity $\dot{\gamma}_\mathrm{d} > 0$ while simultaneously driving it to a desired position z_od over the pole surface, and maintaining it perpendicular to the pole. The design of a feedback model-based control for the representation (1)–(5) is a challenging problem from the nonlinear control point of view. Some of the main difficulties are listed below.

- The kinematic constraints (3)–(5) are completely nonholonomic [13, p. 320]. Moreover, the relative grow vector of the associated control system is (2,1,2), and thus it cannot be transformed into a chained form [23, p. 319].
- The dynamic model (1)–(2) is underactuated, and in the simplest case the shape coordinates are not actuated, hence the result of [24] cannot be directly applied. In the remaining cases, the inertia matrices depend on both actuated and unactuated coordinates.
- Because the system trajectories must satisfy the nonholonomic constraints (3)–(5), it is not clear whether it is possible to induce a periodic motion within the unactuated coordinates fulfilling the control objective stated above, which is a crucial step to apply the methodology of [25], [26].
- Due to the nonholonomic nature of the system, the control objective cannot be translated into a regulation problem, but tracking on the unactuated coordinates must be ensured, for which the result of [27] does not apply.

III. MAIN RESULT

Let the input $\boldsymbol{u}$ be defined as

$$\boldsymbol{u} = \boldsymbol{M}_\mathrm{p} \left(\boldsymbol{P}_\mathrm{h} \boldsymbol{u}_\mathrm{P} + \boldsymbol{Q}_\mathrm{h} \boldsymbol{u}_\mathrm{Q} \right) , \tag{10}$$

where $\boldsymbol{u}_\mathrm{P}$ and $\boldsymbol{u}_\mathrm{Q}$ are two independent inputs belonging to orthogonal subspaces. Since $\boldsymbol{M}_\mathrm{p}$ is always invertible, one can solve (2) for $\ddot{\boldsymbol{q}}_\mathrm{p}$ with the input defined as in (10) to obtain[2]

$$\boldsymbol{M}_\mathrm{r} \ddot{\boldsymbol{q}}_\mathrm{h} + \boldsymbol{c}_\mathrm{r} = -\boldsymbol{T}_\mathrm{h} \boldsymbol{u}_\mathrm{P} , \tag{11}$$

where

$$\boldsymbol{M}_\mathrm{r} = \boldsymbol{M}_\mathrm{h} - \boldsymbol{T}_\mathrm{h} \boldsymbol{M}_\mathrm{p}^{-1} \boldsymbol{T}_\mathrm{h}^\mathrm{T} \tag{12}$$

$$\boldsymbol{c}_\mathrm{r} = \boldsymbol{c}_\mathrm{h} - \boldsymbol{T}_\mathrm{h} \boldsymbol{M}_\mathrm{p}^{-1} \boldsymbol{c}_\mathrm{p} . \tag{13}$$

Now, we define the noncollocated partial feedback linearization (NPFL) [14] input

$$\boldsymbol{u}_\mathrm{P} = -\boldsymbol{T}_\mathrm{h}^{+} \left(\boldsymbol{c}_\mathrm{r} + \boldsymbol{M}_\mathrm{r} \boldsymbol{v}_\mathrm{P} \right) , \tag{14}$$

[2]Notice that by effect of the projection, the input $\boldsymbol{u}_\mathrm{Q}$ does not affect the $\ddot{\boldsymbol{q}}_\mathrm{h}$ dynamics.

and since $\boldsymbol{M}_\mathrm{r}$ is always full rank [28] we obtain

$$\ddot{\boldsymbol{q}}_\mathrm{h} = \boldsymbol{v}_\mathrm{P} , \tag{15}$$

with zero dynamics given in (35).

The control objective consists in designing the input $\boldsymbol{v}_\mathrm{P}$ to drive $\dot{\gamma} \to \dot{\gamma}_\mathrm{d}$ and $(z_\mathrm{o}, \psi, \phi) \to (z_\mathrm{od}, 0, 0)$, while satisfying the nonholonomic constraints (3)–(5).

To design the control strategy, first define

$$\boldsymbol{\xi} = \begin{bmatrix} \xi_1 \\ \xi_2 \\ \xi_3 \end{bmatrix} = \begin{bmatrix} z_\mathrm{o} - z_\mathrm{od} \\ -l_\mathrm{h} s_\phi \\ l_\mathrm{h} c_\phi s_\psi \end{bmatrix} , \tag{16}$$

whose time derivative is given by

$$\dot{\boldsymbol{\xi}} = \begin{bmatrix} \dot{\xi}_1 \\ \dot{\xi}_2 \\ \dot{\xi}_3 \end{bmatrix} = \begin{bmatrix} \xi_2 \dot{\gamma} \\ \xi_3 \dot{\gamma} \\ l_\mathrm{h} s_\phi s_\psi^2 \dot{\gamma} + l_\mathrm{h} c_\phi c_\psi \dot{\psi} \end{bmatrix} . \tag{17}$$

Now, consider the following auxiliary definitions

$$\boldsymbol{\eta} = \begin{bmatrix} \eta_1 \\ \eta_2 \end{bmatrix} = \begin{bmatrix} \dot{\gamma} - \dot{\gamma}_\mathrm{d} \\ \dot{\psi} - f_\psi \end{bmatrix} , \tag{18}$$

where

$$f_\psi \triangleq f_\psi(\psi, \phi, \dot{\gamma}, \boldsymbol{\xi}) = -\left(l_\mathrm{h} s_\phi s_\psi^2 + \boldsymbol{k}_\xi^\mathrm{T} \boldsymbol{\xi} \right) \dot{\gamma} / \left(l_\mathrm{h} c_\phi c_\psi \right) , \tag{19}$$

defined for $-\pi/2 < \phi, \psi < \pi/2$, with $\boldsymbol{k}_\xi = \begin{bmatrix} k_{\xi 1} & k_{\xi 2} & k_{\xi 3} \end{bmatrix}^\mathrm{T}$ a vector of positive constant gains. By substituting (18) into (17) yields

$$\dot{\boldsymbol{\xi}} = \begin{bmatrix} \xi_2 \dot{\gamma}_\mathrm{d} + \xi_2 \eta_1 \\ \xi_3 \dot{\gamma}_\mathrm{d} + \xi_3 \eta_1 \\ -\boldsymbol{k}_\xi^\mathrm{T} \boldsymbol{\xi} \dot{\gamma}_\mathrm{d} - \boldsymbol{k}_\xi^\mathrm{T} \boldsymbol{\xi} \eta_1 + l_\mathrm{h} c_\phi c_\psi \eta_2 \end{bmatrix} . \tag{20}$$

To analyze the resulting dynamics, first define the state

$$\boldsymbol{\zeta} \triangleq \left[\boldsymbol{\xi} \, ; \, \boldsymbol{\eta} \right] . \tag{21}$$

Proposition 3.1: *Define the region* $B_\mathrm{r} \triangleq \{ \boldsymbol{\zeta} : \| \boldsymbol{\zeta} \| \leq l_\mathrm{h} \}$ *and let the control law be given by*

$$\boldsymbol{v}_\mathrm{P} = \begin{bmatrix} v_{\mathrm{P}1} \\ v_{\mathrm{P}2} \end{bmatrix} = \begin{bmatrix} -k_{\eta 1} \eta_1 \\ \frac{\mathrm{d}}{\mathrm{d}t} f_\psi - k_{\eta 2} \eta_2 \end{bmatrix} , \tag{22}$$

where $k_{\eta 1}, k_{\eta 2}$ *are positive constant gains. There exists a bounded region* $B_\delta \subset B_\mathrm{r}$*, and a combination of gains* $\boldsymbol{k}_\xi, k_{\eta 1}, k_{\eta 2}$ *in (19) and (22), such that if the initial condition satisfies* $\boldsymbol{\zeta}(t_0) \in B_\delta$*, then* $\boldsymbol{\zeta}(t) \in B_\mathrm{r} , \forall t \geq t_0$*. Furthermore, the system trajectories are ultimately bounded within an arbitrarily small region* $B_\mu \subset B_\mathrm{r}$*, centered at the origin.* □

Proof 1: First, notice that if $\boldsymbol{\eta} = \boldsymbol{0}$ in (20) one gets

$$\dot{\boldsymbol{\xi}} = \begin{bmatrix} 0 & 1 & 0 \\ 0 & 0 & 1 \\ -k_{\xi 1} & -k_{\xi 2} & -k_{\xi 3} \end{bmatrix} \boldsymbol{\xi} \triangleq \boldsymbol{A}_\xi \boldsymbol{\xi} , \tag{23}$$

which is a linear time-invariant system with $\boldsymbol{A}_\xi$ Hurwitz. By a well-established result of linear control [29, Theorem 4.6] there exist two symmetric positive definite matrices $\boldsymbol{P}_\xi \in \mathbb{R}^3$ and $\boldsymbol{Q}_\xi \in \mathbb{R}^3$ satisfying the Lyapunov equation

$$\boldsymbol{A}_\xi^\mathrm{T} \boldsymbol{P}_\xi + \boldsymbol{P}_\xi \boldsymbol{A}_\xi = -\boldsymbol{Q}_\xi . \tag{24}$$

These matrices fulfill the bounds $\lambda_{\mathrm{Pm}}\|\boldsymbol{x}\|^2 \leq \boldsymbol{x}^{\mathrm{T}}\boldsymbol{P}_{\xi}\boldsymbol{x} \leq \lambda_{\mathrm{PM}}\|\boldsymbol{x}\|^2$ and $\lambda_{\mathrm{Qm}}\|\boldsymbol{x}\|^2 \leq \boldsymbol{x}^{\mathrm{T}}\boldsymbol{Q}_{\xi}\boldsymbol{x} \leq \lambda_{\mathrm{QM}}\|\boldsymbol{x}\|^2$ for every $\boldsymbol{x} \in \mathbb{R}^3$, with $0 < \lambda_{\mathrm{Pm}} \leq \lambda_{\mathrm{PM}}$, and $0 < \lambda_{\mathrm{Qm}} \leq \lambda_{\mathrm{QM}}$, where we denote by λ_{Hm} and λ_{HM} the minimum and the maximum eigenvalue, respectively, of a generic matrix $\boldsymbol{H}$. Now, consider the positive definite function

$$V = \boldsymbol{\xi}^{\mathrm{T}}\boldsymbol{P}_{\xi}\boldsymbol{\xi} + \frac{1}{2}\boldsymbol{\eta}^{\mathrm{T}}\boldsymbol{\eta}\,, \tag{25}$$

which satisfies the bounds

$$\lambda_{\mathrm{Vm}}\|\boldsymbol{\zeta}\|^2 \leq V(\boldsymbol{\zeta}) \leq \lambda_{\mathrm{VM}}\|\boldsymbol{\zeta}\|^2\,, \tag{26}$$

where $\lambda_{\mathrm{Vm}} = \min\{1, \lambda_{\mathrm{Pm}}\}$ and $\lambda_{\mathrm{VM}} = \max\{1, \lambda_{\mathrm{PM}}\}$. Define a region $B_{\delta} \triangleq \left\{\boldsymbol{\zeta} : \|\boldsymbol{\zeta}\| < \sqrt{\frac{\lambda_{\mathrm{Vm}}}{\lambda_{\mathrm{VM}}}}l_{\mathrm{h}}\right\}$ and assume that the initial condition fulfills $\boldsymbol{\zeta}(t_0) \in B_{\delta}$. Notice that, since $(\lambda_{\mathrm{Vm}}/\lambda_{\mathrm{VM}}) \leq 1$, B_{δ} is a subset of B_{r}.

Taking the time derivative of V along the system trajectories yields

$$\dot{V} = -(\dot{\gamma}_{\mathrm{d}} + \eta_1)\boldsymbol{\xi}^{\mathrm{T}}\boldsymbol{Q}_{\xi}\boldsymbol{\xi} + 2\boldsymbol{\xi}^{\mathrm{T}}\boldsymbol{P}_{\xi}\boldsymbol{b}\eta_2 + \eta_1\dot{\eta}_1 + \eta_2\dot{\eta}_2\,, \tag{27}$$

where $\boldsymbol{b} = \begin{bmatrix}0 & 0 & l_{\mathrm{h}}c_{\phi}c_{\psi}\end{bmatrix}^{\mathrm{T}}$. By taking into account (15) and (18) and substituting the control law (22) yields

$$\dot{V} = -\dot{\gamma}_{\mathrm{d}}\boldsymbol{\xi}^{\mathrm{T}}\boldsymbol{Q}_{\xi}\boldsymbol{\xi} - \eta_1\boldsymbol{\xi}^{\mathrm{T}}\boldsymbol{Q}_{\xi}\boldsymbol{\xi} - k_{\eta 1}\eta_1^2 + 2\eta_2\boldsymbol{\xi}^{\mathrm{T}}\boldsymbol{P}_{\xi}\boldsymbol{b} - k_{\eta 2}\eta_2^2\,. \tag{28}$$

In the set B_{r} this function can be upper bounded by

$$\begin{aligned}\dot{V} \leq & -\dot{\gamma}_{\mathrm{d}}\boldsymbol{\xi}^{\mathrm{T}}\boldsymbol{Q}_{\xi}\boldsymbol{\xi} + \lambda_{\mathrm{QM}}l_{\mathrm{h}}^2|\eta_1| - k_{\eta 1}|\eta_1|^2 \\ & + 2\lambda_{\mathrm{PM}}l_{\mathrm{h}}^2|\eta_2| - k_{\eta 2}|\eta_2|^2 \\ \leq & -\dot{\gamma}_{\mathrm{d}}\lambda_{\mathrm{Qm}}\|\boldsymbol{\xi}\|^2 - |\eta_1|\left(k_{\eta 1}|\eta_1| - \lambda_{\mathrm{QM}}l_{\mathrm{h}}^2\right) \\ & - |\eta_2|\left(k_{\eta 2}|\eta_2| - 2\lambda_{\mathrm{PM}}l_{\mathrm{h}}^2\right) \\ = & -\dot{\gamma}_{\mathrm{d}}\lambda_{\mathrm{Qm}}\|\boldsymbol{\zeta}\|^2 - |\eta_1|\left(\left(k_{\eta 1} - \dot{\gamma}_{\mathrm{d}}\lambda_{\mathrm{Qm}}\right)|\eta_1| - \lambda_{\mathrm{QM}}l_{\mathrm{h}}^2\right) \\ & - |\eta_2|\left(\left(k_{\eta 2} - \dot{\gamma}_{\mathrm{d}}\lambda_{\mathrm{Qm}}\right)|\eta_2| - 2\lambda_{\mathrm{PM}}l_{\mathrm{h}}^2\right)\,,\end{aligned} \tag{29}$$

since $\|\boldsymbol{\zeta}\|^2 = \|\boldsymbol{\xi}\|^2 + |\eta_1|^2 + |\eta_2|^2$. Notice that the term $-|\eta_1|\left(\left(k_{\eta 1} - \dot{\gamma}_{\mathrm{d}}\lambda_{\mathrm{Qm}}\right)|\eta_1| - \lambda_{\mathrm{QM}}l_{\mathrm{h}}^2\right)$ is zero for $|\eta_1| = 0$ and negative for $|\eta_1| > \lambda_{\mathrm{QM}}l_{\mathrm{h}}^2/\left(k_{\eta 1} - \dot{\gamma}_{\mathrm{d}}\lambda_{\mathrm{Qm}}\right)$, so by continuity there must exist a maximum for $|\eta_1|$. This maximum can be easily verified to be at $|\eta_1|_{\max} = \lambda_{\mathrm{QM}}l_{\mathrm{h}}^2/\left(2\left(k_{\eta 1} - \dot{\gamma}_{\mathrm{d}}\lambda_{\mathrm{Qm}}\right)\right)$. Similar arguments can be used for the last term of (29). Overall, one has

$$\dot{V} \leq -\dot{\gamma}_{\mathrm{d}}\lambda_{\mathrm{QM}}\|\boldsymbol{\zeta}\|^2 + c_{\eta 1} + c_{\eta 2}\,, \tag{30}$$

where $c_{\eta 1} \triangleq \lambda_{\mathrm{QM}}^2 l_{\mathrm{h}}^4/\left(2\left(k_{\eta 1} - \dot{\gamma}_{\mathrm{d}}\lambda_{\mathrm{Qm}}\right)\right)$ and $c_{\eta 2} \triangleq 2\lambda_{\mathrm{PM}}^2 l_{\mathrm{h}}^4/\left(\left(k_{\eta 2} - \dot{\gamma}_{\mathrm{d}}\lambda_{\mathrm{Qm}}\right)\right)$, with $k_{\eta 1}, k_{\eta 2} > \dot{\gamma}_{\mathrm{d}}\lambda_{\mathrm{Qm}}$. Therefore $\dot{V} \leq 0$ for

$$\|\boldsymbol{\zeta}\| \geq \sqrt{\left(c_{\eta 1} + c_{\eta 2}\right)/\left(\dot{\gamma}_{\mathrm{d}}\lambda_{\mathrm{Qm}}\right)} \triangleq \mu\,, \tag{31}$$

and thus the system trajectories are ultimately bounded by a region $B_{\mu} \triangleq \{\boldsymbol{\zeta} : \|\boldsymbol{\zeta}\| \leq \mu\}$. Since $k_{\eta 1}$ and $k_{\eta 2}$ can be chosen freely, the ultimate bound radius μ can be driven arbitrarily small. Furthermore, μ can be easily forced to satisfy

$$\mu < \sqrt{\frac{\lambda_{\mathrm{Vm}}}{\lambda_{\mathrm{VM}}}}l_{\mathrm{h}}\,, \tag{32}$$

in order to guarantee $B_{\mu} \subset B_{\mathrm{r}}$.

There is a circularity in the proof[3] because when obtaining (29) it is implicitly assumed that $\boldsymbol{\zeta} \in B_{\mathrm{r}}, \forall t \geq t_0$. To show that this is indeed the case, first notice that $\|\boldsymbol{\zeta}(t_0)\| \in B_{\delta} \implies \|\boldsymbol{\zeta}(t_0)\| < \sqrt{\frac{\lambda_{\mathrm{Vm}}}{\lambda_{\mathrm{VM}}}}l_{\mathrm{h}} \leq l_{\mathrm{h}}$. Suppose that $\boldsymbol{\zeta}$ leaves B_{r}, so by continuity there must exist a time $T > t_0$ such that $\|\boldsymbol{\zeta}(T)\| = l_{\mathrm{h}}$. Notice that in order to leave B_{r}, the trajectories cannot enter in B_{μ}, since this set is positively invariant because $\dot{V} \leq 0$ in its frontier. Therefore, the trajectories must remain in $B_{\mathrm{r}} \backslash B_{\mu}$ before leaving B_{r}. On one hand, since $\dot{V} \leq 0$ for $t \in [t_0, T)$, and after (26), we have

$$V(\boldsymbol{\zeta}(T)) \leq V(\boldsymbol{\zeta}(t_0)) < \lambda_{\mathrm{Vm}}l_{\mathrm{h}}^2\,. \tag{33}$$

On the other hand, from the assumption $\boldsymbol{\zeta}(T) = l_{\mathrm{h}}$ and (26), one has

$$V(\boldsymbol{\zeta}(T)) = V(l_{\mathrm{h}}) \geq \lambda_{\mathrm{Vm}}l_{\mathrm{h}}^2\,. \tag{34}$$

By noticing that (33) and (34) are in contradiction, we can conclude that the original assumption is incorrect, and thus $\boldsymbol{\zeta}$ must remain in B_{r}.

Notice that in the interior of B_{r}, after (16) and (18), $\boldsymbol{\zeta} \approx \boldsymbol{0}$ implies $(z_{\mathrm{o}}, \phi, \psi) \approx (z_{\mathrm{od}}, 0, 0)$ and $\dot{\gamma} \approx \dot{\gamma}_{\mathrm{d}}$, satisfying the control objective.

Remark 1: For simplicity's sake, we have chosen the upper-bound for the state $\boldsymbol{\zeta}$, which defines the region B_{r} in Proposition 3.1, to be l_{h}. This choice makes the stability proof clearer yet it is very conservative. Nevertheless, notice that this bound is arbitrary and can be modified to enlarge the domain of attraction of the controller. ■

To design a control strategy to stabilize the pole dynamics, we assume that the hoop has reached stationary state, so that $\ddot{\boldsymbol{q}}_{\mathrm{h}} \equiv \boldsymbol{0}$. From (1)–(2) and (10) one gets

$$\ddot{\boldsymbol{q}}_{\mathrm{p}} = \boldsymbol{f}_{\mathrm{p}} + \boldsymbol{f}_{\mathrm{uP}} + \boldsymbol{Q}_{\mathrm{h}}\boldsymbol{u}_{\mathrm{Q}}\,, \tag{35}$$

where $\boldsymbol{f}_{\mathrm{p}} = \boldsymbol{M}_{\mathrm{p}}^{-1}\boldsymbol{c}_{\mathrm{p}}$ and $\boldsymbol{f}_{\mathrm{uP}} = \boldsymbol{P}_{\mathrm{h}}\boldsymbol{u}_{\mathrm{P}}$.

As discussed in Section II, investigating the controllability of the nonlinear system (35) is a very difficult task. For this reason, only a local result will be pursued, based on the linearization of (35) around its nominal trajectories

$$\boldsymbol{q}^* \triangleq \begin{bmatrix}\dot{\gamma}_{\mathrm{d}}t & 0 & z_{\mathrm{od}} & (l_{\mathrm{h}}/r_{\mathrm{p}})\dot{\gamma}_{\mathrm{d}}t & 0 & \boldsymbol{q}_{\mathrm{p}}^{*\mathrm{T}}\end{bmatrix}^{\mathrm{T}} \tag{36}$$

$$\dot{\boldsymbol{q}}^* \triangleq \begin{bmatrix}\dot{\gamma}_{\mathrm{d}} & 0 & 0 & (l_{\mathrm{h}}/r_{\mathrm{p}})\dot{\gamma}_{\mathrm{d}} & 0 & \dot{\boldsymbol{q}}_{\mathrm{p}}^{*\mathrm{T}}\end{bmatrix}^{\mathrm{T}}\,, \tag{37}$$

where $\boldsymbol{q}_{\mathrm{p}}^*$ is the pole coordinates nominal trajectories vector, and depends on the pole degrees of freedom. Only two of the study cases are analyzed here: (i) three Cartesian directions of movement along the x_{w}, y_{w}, and z_{w} inertial frame axes[4] and (ii) two Cartesian degree-of-freedom along x_{w} and y_{w}, and two rotations around the same axes. The configuration coordinates for the three Cartesian degree-of-freedom case are the pole center of mass coordinates $(o_{\mathrm{px}}, o_{\mathrm{py}}, o_{\mathrm{pz}})$. For the latter case, the rotation matrix of the pole with respect to the inertial frame is given by the composition of two basic rotation matrices, namely

$$\boldsymbol{R}_{\mathrm{h}} = \boldsymbol{R}_x(\alpha_1)\boldsymbol{R}_y(\alpha_2)\,, \tag{38}$$

[3]See [30], remarks on Theorem 5.3.1.

[4]This is the configuration studied in [12].

and thus the configuration coordinates for the pole are $(o_{\mathrm{px}}, o_{\mathrm{py}}, \alpha_1, \alpha_2)$. Therefore, the nominal trajectories for the pole in both cases are $\boldsymbol{q}_{\mathrm{p}}^* = \dot{\boldsymbol{q}}_{\mathrm{p}}^* = \mathbf{0}_m$.

By defining the state space coordinates $\boldsymbol{x} \triangleq \left[\boldsymbol{q}_{\mathrm{p}}\,;\,\dot{\boldsymbol{q}}_{\mathrm{p}}\right]$, we obtain the following linearized model

$$\dot{\boldsymbol{x}} = \boldsymbol{A}(t)\boldsymbol{x} + \boldsymbol{B}(t)\boldsymbol{u}_{\mathrm{Q}}\,, \tag{39}$$

where

$$\boldsymbol{A}(t) = \begin{bmatrix} \boldsymbol{O} & \boldsymbol{I} \\ \boldsymbol{a}_{21}(t) & \boldsymbol{a}_{22}(t) \end{bmatrix} \tag{40}$$

$$\boldsymbol{B}(t) = \boldsymbol{Q}_{\mathrm{h}}|_{\boldsymbol{q}^*,\dot{\boldsymbol{q}}^*} \tag{41}$$

$$\boldsymbol{a}_{21}(t) = \frac{\partial \boldsymbol{f}_{\mathrm{p}}}{\partial \boldsymbol{q}_{\mathrm{p}}}|_{\boldsymbol{q}^*,\dot{\boldsymbol{q}}^*} \tag{42}$$

$$\boldsymbol{a}_{22}(t) = \frac{\partial \boldsymbol{f}_{\mathrm{p}}}{\partial \dot{\boldsymbol{q}}_{\mathrm{p}}}|_{\boldsymbol{q}^*,\dot{\boldsymbol{q}}^*}\,. \tag{43}$$

Notice that for carrying out the linearization, the term $\boldsymbol{f}_{\mathrm{uP}}$ in (35) is considered as an external bounded input. It can be shown that the periodic linear time-varying system (39) is *not controllable* [31, Theorem 6.11] for the three pole Cartesian inputs case, but it is *controllable* [31, Theorem 6.12] for the two translations-two rotations pole inputs case. For this last case, it is possible to find a stabilizing controller of the form [32]

$$\boldsymbol{u}_{\mathrm{Q}} = -\boldsymbol{\Gamma}^{-1}\boldsymbol{B}^{\mathrm{T}}(t)\boldsymbol{R}(t)\boldsymbol{x}\,, \tag{44}$$

where $\boldsymbol{R}(t) \in \mathbb{R}^{8\times 8}$ is a symmetric positive definite matrix which satisfies the Riccati equation

$$\dot{\boldsymbol{R}}(t) + \boldsymbol{A}^{\mathrm{T}}(t)\boldsymbol{R}(t) + \boldsymbol{R}(t)\boldsymbol{A}(t) + \boldsymbol{G} = \boldsymbol{R}(t)\boldsymbol{B}(t)\boldsymbol{\Gamma}^{-1}\boldsymbol{B}^{\mathrm{T}}(t)\boldsymbol{R}(t)\,, \tag{45}$$

with $\boldsymbol{G} \in \mathbb{R}^{8\times 8}$ and $\boldsymbol{\Gamma} \in \mathbb{R}^{4\times 4}$ positive definite matrices of constant gains. An approximation for the solution of the Riccati equation (45) can be found by employing the *quasi–linearization of the periodic Riccati equation* method [33, p. 137].

Conditions for maintaining contact

For the modeling and control design presented in the above sections we have assumed rolling without slipping between the objects surfaces. Intuitively speaking, one can argue that there must be a minimal spinning speed for the hoop in order to not losing contact with the pole. To get an idea of the magnitude of this minimum speed, assume that stationary state has reached, *i.e.,* the hoop is spinning in the orthogonal plane to the pole main axis. The computation of the Lagrange multipliers from the Lagrange-d'Alembert formulation, which was used to obtain the model (1)–(2), can be employed to compute the internal forces [13, p. 279]. A straightforward calculation of the radial component gives the contact condition

$$m_{\mathrm{h}} l_{\mathrm{h}} \dot{\theta}^2 - m_{\mathrm{h}} g_0 > 0\,, \tag{46}$$

which is just the difference between the centripetal and gravity forces acting on the hoop, with g_0 the gravity acceleration constant. Since this minimum velocity is intended for the best scenario (the hoop perpendicular to the pole), the desired velocity and the initial conditions should fulfill $\dot{\theta} >> \sqrt{g_0/l_{\mathrm{h}}}$. For the case when the pole is in vertical position the contact keeping depends on the static friction between the surfaces, hence the desired and initial condition for the spinning speed must satisfy $\dot{\theta} >> \sqrt{g_0/\left(f_{\mathrm{c}} l_{\mathrm{h}}\right)}$, where f_{c} is the static friction coefficient. On the other hand, the upper limit for the spinning speed depends on the bandwidth of the system, which is mainly limited by the signals acquisition and processing time, and the actuators maximum speed and acceleration.

Remark 2: As an assumption for maintaining contact as well as to fulfill the requirements of Proposition 3.1, the desired hoop spinning velocity $\dot{\gamma}_{\mathrm{d}}$ must be sufficiently close to the initial velocity $\dot{\gamma}$, which in turn must be strictly greater than zero. For simplicity's sake we consider the initial swing controller, to obtain this initial spinning, out of the scope of this paper, although it can be induced by some planar-motion open-loop controller, *e.g.* the one proposed in [34]. ■

Discussion on the generalization of the results

Although the problem addressed in this work is a particular case study, the dynamic model (1)–(2) represents a more general class of underactuated mechanical systems. For this, consider $\boldsymbol{q}_{\mathrm{h}} \in \mathbb{R}^k$ with $m > k$, *i.e.* the input vector dimension is greater than the underactuated coordinates dimension. As mentioned in Section II, the system is strongly inertially coupled if the matrix $\boldsymbol{T}_{\mathrm{h}}(\boldsymbol{q})$ has rank k, and thus the well-known NPFL method can be employed. The key property exploited in this work arises in the case when the dimension of the column space of $\boldsymbol{T}_{\mathrm{h}}(\boldsymbol{q})$ is strictly greater than k. In this case one can construct the projection matrices (7)–(8) to decouple the system directions of motion into two orthogonal subspaces before applying the NPFL technique. While the evolution of the underactuated coordinates is exactly the same as with the direct application of NPFL, there are still control directions on the zero dynamics. As shown in the case study, this zero dynamics can be unstable but stabilizable when using the proposed projectors.

To design a controller for the underactuated coordinates subjected to nonholonomic constraints, the backstepping technique is employed, which is a natural tool to deal with these kind of systems, as has been shown in [35], [36]. The remaining coordinates controllability can be studied by means of the several tools currently available in the literature. Due to the complexity of the present case study, here we have employed a linearization around the periodic nominal trajectories to show controllability, and a quasi-linearization of the periodic Riccati equation to design a controller for practical stabilization of the actuated coordinates. However, in principle any valid tool can be employed to deal with this subsystem.

Potential applications of the current approach include underactuated mechanical systems subjected to nonholonomic constraints, with unstable zero dynamics when employing NPFL, and with coupling inertia matrix column rank greater than the underactuated coordinates dimension. Examples of such systems could be the non-planar generalizations of the drone-driven ball and beam [37] and the devil stick [38].

IV. SIMULATION

In this section we present the results of a numerical simulation carried out to test the validity of the approach. The parameters employed for the simulation are listed in Table I. The corresponding matrices and vectors in (1)–(2) were obtained by means of a symbolic computing software (*Wolfram Mathematica*) and are not included here due to space constraint. For the pole not to be affected by the hoop motion we assume that the pole apparent inertia can be assigned by the manipulator *e.g.,* as proposed in [39], so the pole actual mass must not have to be large, but only its apparent inertia. It is considered that the pole sample time is $T = 0.005\,\mathrm{s}$, while the hoop coordinates are measured by means of a vision system with sample time $T_\mathrm{v} = 0.02\,\mathrm{s}$. An animation video is included as an attachment to have a better visualization of the simulation results.

TABLE I
SIMULATION PARAMETERS

Meaning	Parameter	Value
Hoop mass	m_h	$0.05\,\mathrm{kg}$
Pole mass	m_p	$10\,\mathrm{kg}$
Hoop radius	l_h	$0.3\,\mathrm{m}$
Hoop thickness radius	r_h	$0.005\,\mathrm{m}$
Pole radius	r_p	$0.025\,\mathrm{m}$
Pole length	l_p	$0.7\,\mathrm{m}$
Gravity constant	g_0	$9.81\,\mathrm{m/s^2}$

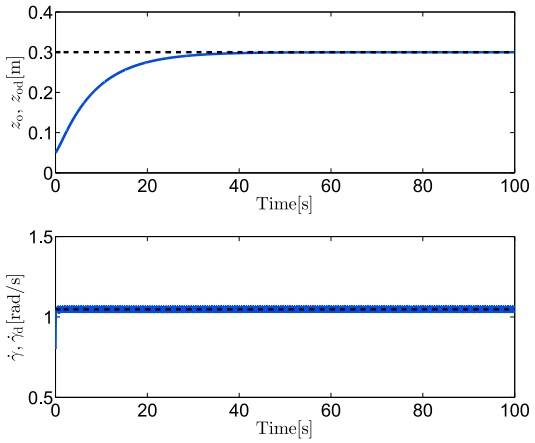

Fig. 2. Contact coordinates evolution: real (—), desired (- - -).

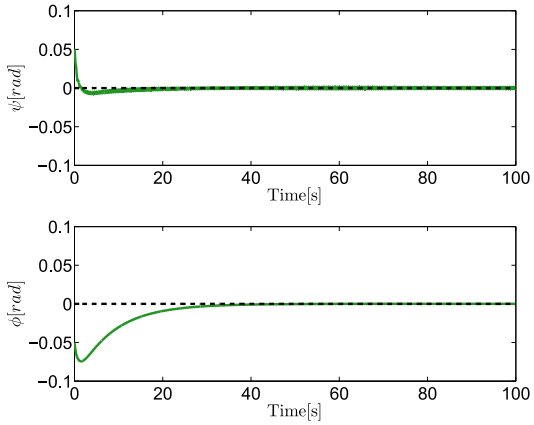

Fig. 3. Asymptotic stabilization of the ψ and ϕ coordinates.

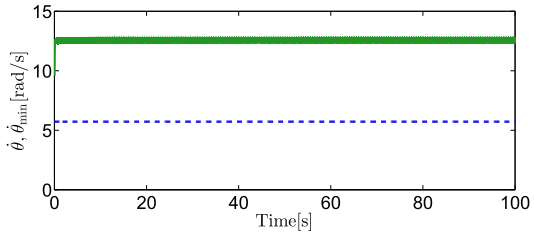

Fig. 4. Evolution of $\dot\theta$ (—) and the minimum value required to maintain contact (- - -).

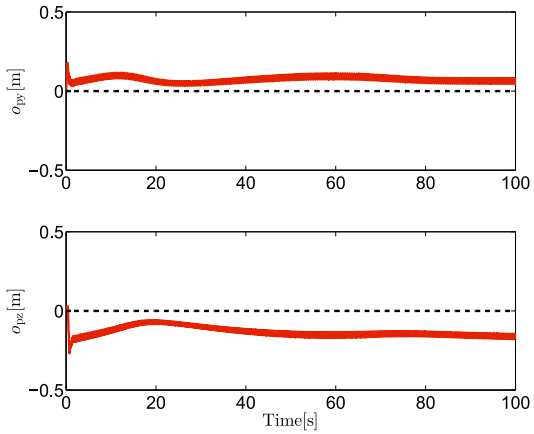

Fig. 5. Pole Cartesian coordinates with respect to the initial position.

The desired coordinates are $\dot\gamma_\mathrm{d} = 4\pi r_\mathrm{p}/l_\mathrm{h} \approx 1.0472\,\mathrm{rad/s}$ and $z_\mathrm{od} = 0.3\,\mathrm{m}$. The gains for the LQR controller in (44)–(45) are chosen as $\boldsymbol{\Gamma} = \mathrm{diag}\{0.5, 0.5, 1, 1\}$ and $\boldsymbol{G} = \mathrm{diag}\{200, 200, 40000, 40000, 10, 10, 4, 4\}$. The boundary condition for approximating $\boldsymbol{R}(t)$ is chosen as $\boldsymbol{R}(T_\mathrm{s}) = \boldsymbol{O}_{8\times 8}$, where T_s is the period of the linearized system (39), which is given by $T_\mathrm{s} = (l_\mathrm{h}/r_\mathrm{p})\dot\gamma_\mathrm{d}$. The hoop controller gains are chosen as $k_{\eta 1} = 20$, $k_{\eta 2} = 10$, $k_{\xi 1} = 40$, $k_{\xi 2} = 40$, and $k_{\xi 3} = 4$. The initial conditions for the generalized positions are set to $\gamma(t_0) = 0\,\mathrm{rad}$, $\psi(t_0) = 0.05\,\mathrm{rad}$, $z_\mathrm{o}(t_0) = 0.05\,\mathrm{m}$, $\theta(t_0) = \pi\,\mathrm{rad}$, and $\phi(t_0) = -0.05\,\mathrm{rad}$, while the initial conditions for the velocities are set to $\dot\gamma(t_0) = 0.8\,\mathrm{rad/s}$, $\dot\psi(t_0) = 0\,\mathrm{rad/s}$, $\dot z_\mathrm{o}(t_0) = -l_\mathrm{h}\sin(\phi(t_0))\dot\gamma(t_0)\,\mathrm{m/sec}$, $\dot\theta(t_0) = l_\mathrm{h}\cos(\phi(t_0))\dot\gamma(t_0)/r_\mathrm{p}\,\mathrm{rad/s}$, and $\dot\phi(t_0) = -\sin(\psi(t_0))\dot\gamma(t_0)\,\mathrm{rad/s}$.

The time evolution of the contact coordinates is shown in Fig. 2, where it can be seen that the control objective is satisfied. In Fig. 3 the graph of the ψ and ϕ coordinates is displayed, showing their ultimately boundedness within a small region around the origin. The time evolution of the $\dot\theta$ coordinate is displayed in Fig. 4, along with the minimum speed required to maintain contact. It can be seen that this condition is satisfied during all the simulation time with a considerably large margin. The Cartesian coordinates of the pole center of mass are shown in Fig. 5, while the time evolution of the two angles describing the pole orientation is

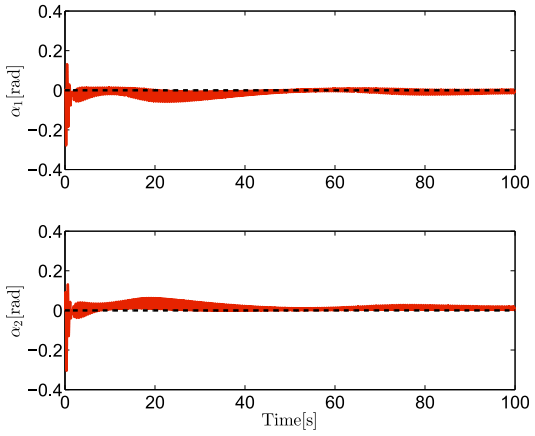

Fig. 6. Stabilization of the pole rotation angles.

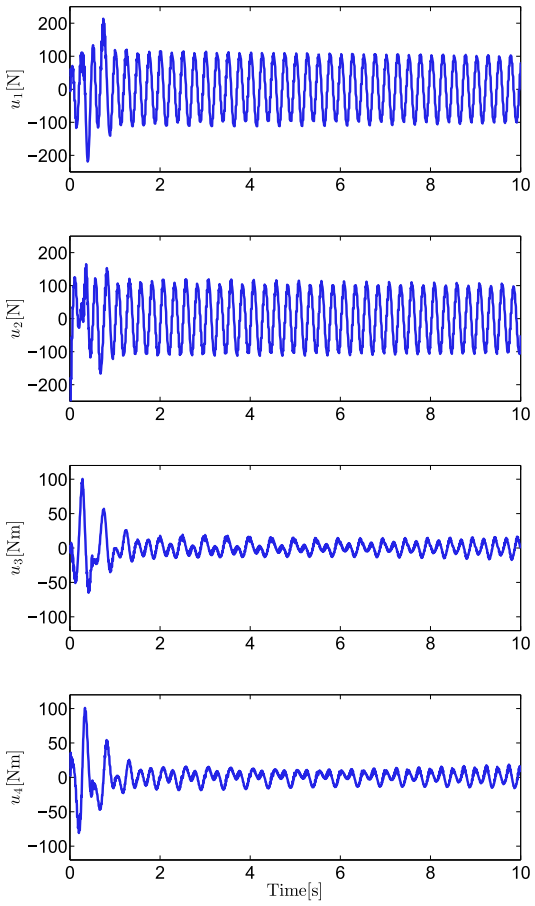

Fig. 7. Force and torque inputs on the pole.

shown in Fig. 6. In these figures, it can be seen that all the pole coordinates are stabilized by the proposed controller. Finally, the control inputs, *i.e.* the forces and torques acting on the pole, for the first 10 seconds of the simulation are shown in Figure 7.

V. CONCLUSIONS AND FUTURE WORK

In this work we have addressed the problem of a robotic hula-hoop system, which is an underactuated mechanical system subject to second order nonholonomic constraints. For this system we designed a locally stable controller scheme by exploiting the null space of the inertia coupling matrices, making it possible to simultaneously satisfy the control objective of spinning the hoop at a desired angular velocity on a desired position over the pole surface and to stabilize the pole coordinates. We developed a formal proof which guarantees locally ultimate boundedness of the hoop coordinates with arbitrary small ultimate bound on the tracking error and boundedness of the pole coordinates. To validate the proposed approach, we presented a numerical simulation which showed the good performance of our solution.

For further research, the structural properties of the system model can be exploited to enlarge the domain of validity of the proposed controller, since at its present form it only guarantees local stability within a rather conservative domain. The same structural properties can be also employed to avoid the dynamic cancellation in the control law so as to render the strategy less dependent on the model accuracy. Another interesting solution to deal with the parametric uncertainties is the Model Predictive Control approach, which has been successfully employed in recent years for the control of nonlinear systems. Finally, it remains to perform an experimental validation. Some of the main challenges for the experimental setup are the necessity of a very fast reconstruction of the hoop position and orientation (in the simulation is was considered to be implemented at a 20 Hz rate) with good resolution, and the high velocities and acceleration required for the actuator (*e.g.,* for the humanoid-like robot used in the simulations).

ACKNOWLEDGMENT

The authors want to thank the anonymous reviewers, whose invaluable comments and suggestions helped to greatly improve this work. The first author wants to thank Andrea Fontanelli for providing the code to make the accompanying animation video.

REFERENCES

[1] K. M. Lynch and M. T. Mason, "Dynamic nonprehensile manipulation: Controllability, planning, and experiments," *The International Journal of Robotics Research*, vol. 18, no. 1, pp. 64–92, 1999.

[2] P. Choudhury and K. M. Lynch, "Rolling manipulation with a single control," *The International Journal of Robotics Research*, vol. 21, no. 5-6, pp. 475–487, 2002.

[3] D. Serra, A. C. Satici, F. Ruggiero, V. Lippiello, and B. Siciliano, "An optimal trajectory planner for a robotic batting task: The table tennis example." in *Proceedings of the 13th International Conference on Informatics in Control, Automation and Robotics (ICINCO)*, 2016, pp. 90–101.

[4] S. Akella and M. T. Mason, "Posing polygonal objects in the plane by pushing," *The International Journal of Robotics Research*, vol. 17, no. 1, pp. 70–88, 1998.

[5] J.-S. Hu, M.-C. Chien, Y.-J. Chang, S.-H. Su, and C.-Y. Kai, "A ball-throwing robot with visual feedback," in *Proceedings of the IEEE/RSJ International Conference on Intelligent Robots and Systems (IROS)*. IEEE, 2010, pp. 2511–2512.

[6] M. Erdmann, "An exploration of nonprehensile two-palm manipulation," *The International Journal of Robotics Research*, vol. 17, no. 5, pp. 485–503, 1998.

[7] V. Lippiello, F. Ruggiero, and B. Siciliano, "The effect of shapes in input-state linearization for stabilization of nonprehensile planar rolling dynamic manipulation," *IEEE Robotics and Automation Letters*, vol. 1, no. 1, pp. 492–499, 2016.

[8] K. M. Lynch, N. Shiroma, H. Arai, and K. Tanie, "The roles of shape and motion in dynamic manipulation: The butterfly example," in *Proceedings of the IEEE International Conference on Robotics and Automation (ICRA)*, vol. 3, Leuven, Belgium, 1998, pp. 1958–1963.

[9] J.-C. Ryu, F. Ruggiero, and K. M. Lynch, "Control of nonprehensile rolling manipulation: Balancing a disk on a disk," *IEEE Transactions on Robotics*, vol. 29, no. 5, pp. 1152–1161, 2013.

[10] A. Donaire, F. Ruggiero, L. R. Buonocore, V. Lippiello, and B. Siciliano, "Passivity-based control for a rolling-balancing system: The nonprehensile disk-on-disk," *IEEE Transactions on Control Systems Technology*, 2016.

[11] J. Nishizaki, S. Nakaura, and M. Sampei, "Modeling and control of hula-hoop system," in *Proceedings of the 48th IEEE Conference on Decision and Control (CDC/CCC 2009)*, Shanghai, China, 2009, pp. 4125–4130.

[12] A. Gutiérrez-Giles, F. Ruggiero, V. Lippiello, and B. Siciliano, "Modelling and control of a robotic hula-hoop system without velocity measurements," in *20th World Congress of the International Federation of Automatic Control (Accepted)*, Toulouse, France, 2017.

[13] R. M. Murray, Z. Li, S. S. Sastry, and S. S. Sastry, *A mathematical introduction to robotic manipulation*. CRC press, 1994.

[14] M. W. Spong, "Partial feedback linearization of underactuated mechanical systems," in *Proceedings of IEEE/RSJ/GI International Conference on Intelligent Robots and Systems (IROS)*, Munich, Germany, 1994, pp. 314–321.

[15] Wolfram Research, Inc., "Mathematica 11." [Online]. Available: https://www.wolfram.com

[16] G. Oriolo and Y. Nakamura, "Control of mechanical systems with second-order nonholonomic constraints: Underactuated manipulators," in *Proceedings of the 30th IEEE Conference on Decision and Control (CDC)*, 1991, pp. 2398–2403.

[17] M. Reyhanoglu, A. van der Schaft, N. H. McClamroch, and I. Kolmanovsky, "Dynamics and control of a class of underactuated mechanical systems," *IEEE Transactions on Automatic Control*, vol. 44, no. 9, pp. 1663–1671, 1999.

[18] R. W. Brockett *et al.*, *Asymptotic stability and feedback stabilization*. Birkhauser, Boston, MA, 1983, vol. 27, no. 1.

[19] H. J. Sussmann *et al.*, "Subanalytic sets and feedback control," *Journal of Differential Equations*, vol. 31, no. 1, pp. 31–52, 1979.

[20] J.-M. Coron, "On the stabilization in finite time of locally controllable systems by means of continuous time-varying feedback law," *SIAM Journal on Control and Optimization*, vol. 33, no. 3, pp. 804–833, 1995.

[21] H. J. Sussmann and V. Jurdjevic, "Controllability of nonlinear systems," *Journal of Differential Equations*, vol. 12, no. 1, pp. 95–116, 1972.

[22] R. Olfati-Saber, "Cascade normal forms for underactuated mechanical systems," in *Proceedings of the 39th IEEE Conference on Decision and Control (CDC)*, vol. 3, 2000, pp. 2162–2167.

[28] Y.-L. Gu and Y. Xu, "A normal form augmentation approach to adaptive control of space robot systems," *Dynamics and Control*, vol. 5, no. 3, pp. 275–294, 1995.

[23] A. De Luca and G. Oriolo, "Modelling and control of nonholonomic mechanical systems," in *Kinematics and dynamics of multi-body systems*. Springer Vienna, 1995, pp. 277–342.

[24] A. Donaire, J. G. Romero, R. Ortega, B. Siciliano, and M. Crespo, "Robust IDA-PBC for underactuated mechanical systems subject to matched disturbances," *International Journal of Robust and Nonlinear Control*, 2016.

[25] A. S. Shiriaev, L. B. Freidovich, and S. V. Gusev, "Transverse linearization for controlled mechanical systems with several passive degrees of freedom," *IEEE Transactions on Automatic Control*, vol. 55, no. 4, pp. 893–906, 2010.

[26] A. S. Shiriaev, L. B. Freidovich, and M. W. Spong, "Controlled invariants and trajectory planning for underactuated mechanical systems," *IEEE Transactions on Automatic Control*, vol. 59, no. 9, pp. 2555–2561, 2014.

[27] A. Donaire, R. Mehra, R. Ortega, S. Satpute, J. G. Romero, F. Kazi, and N. M. Singh, "Shaping the energy of mechanical systems without solving partial differential equations," *IEEE Transactions on Automatic Control*, vol. 61, no. 4, pp. 1051–1056, 2016.

[29] H. Khalil, *Nonlinear systems*, 3rd ed. Prentice-Hall, Englewood Cliffs, NJ, 2002.

[30] M. Vidyasagar, *Nonlinear systems analysis*, 2nd ed. Society for Industrial and Applied Mathematics, Philadelphia, PA, 2002.

[31] C.-T. Chen, *Linear system theory and design*, 3rd ed. Oxford University Press, New York, NY, 1999.

[32] A. Shiriaev, J. W. Perram, and C. Canudas-de Wit, "Constructive tool for orbital stabilization of underactuated nonlinear systems: Virtual constraints approach," *IEEE Transactions on Automatic Control*, vol. 50, no. 8, pp. 1164–1176, 2005.

[33] S. Bittanti, A. J. Laub, and J. C. Willems, *The Riccati equation*, 1st ed. Springer-Verlag, New York, NY, 1991.

[34] A. P. Seyranian and A. O. Belyakov, "How to twirl a hula hoop," *American Journal of Physics*, vol. 79, no. 7, pp. 712–715, 2011.

[35] T. Hamel and C. Samson, "Transverse function control of a motorboat," *Automatica*, vol. 65, pp. 132–139, 2016.

[36] Z.-P. JIANGdagger and H. Nijmeijer, "Tracking control of mobile robots: a case study in backstepping," *Automatica*, vol. 33, no. 7, pp. 1393–1399, 1997.

[37] A. A. Rubio, A. Seuret, Y. Ariba, and A. Mannisi, "Optimal control strategies for load carrying drones," in *Delays and Networked Control Systems*. Springer, 2016, pp. 183–197.

[38] Y. Kawaida, S. Nakaura, R. Ohata, and M. Sampei, "Feedback control of enduring rotary motion of devil stick," in *Proceedings of the 42nd IEEE Conference on Decision and Control (CDC)*, vol. 4. IEEE, 2003, pp. 3396–3401.

[39] F. Ficuciello, L. Villani, and B. Siciliano, "Variable impedance control of redundant manipulators for intuitive human–robot physical interaction," *IEEE Transactions on Robotics*, vol. 31, no. 4, pp. 850–863, 2015.